Hot-wall-epitaxy - the method of choice for the growth of highly ordered organic epilayers

Helmut Sitter [a] , Andrei Andreev [a] , Gebhart Matt [b] & N. S. Sariciftci [b]

[a] Inst. of Semiconductor- and Solid State Physics, Johannes Kepler University Linz, Linz, A-4040, Austria

[b] LIOS and Inst. for Physical Chemistry, Johannes Kepler University Linz, Linz, A-4040, Austria

PLEASE SCROLL DOWN FOR ARTICLE

HOT-WALL-EPITAXY – THE METHOD OF CHOICE FOR THE GROWTH OF HIGHLY ORDERED ORGANIC EPILAYERS

Helmut Sitter* and Andrei Andreev
Johannes Kepler University Linz, Inst. of Semiconductor-
and Solid State Physics, A-4040 Linz, Austria

Gebhart Matt and N. S. Sariciftci
Johannes Kepler University Linz, LIOS and Inst. for Physical
Chemistry, A-4040 Linz, Austria

Hot Wall Epitaxy works close to thermodynamic equilibrium and is therefore most applicable for materials with Van der Waals binding character. The Hot Wall Epitaxy system can be described as semiclosed growth reactor, consisting of a vertically mounted quartz cylinder, which is heated by three separately controllable ovens, and is closed on top by the substrate. The first oven heats the source material and controls the growth rate. The second heats the hot wall between source and substrate, which guaranties the closed character of the reactor and helps to avoid loss of valuable material. The third oven controls the substrate temperature and allows to influence the growth process on the substrate surface.

We achieved crystalline perfection for C_{60} layers on mica substrates and fabricated Ba-doped n-type layers with mobilities of $6000\,cm^2/Vs$ at room temperature.

Keywords: hot wall epitaxy; crystalline C_{60} films; doping; mobility

1. INTRODUCTION

Research on conjugated organic systems is a rapidly expanding field at the turn of chemistry, condensed matter physics, materials science and device physics due to the promising opportunities for applications of these π-electron semiconductors in electronics and photonics. Due to their

*Corresponding author. E-mail: helmut.sitter@jku.at

interdisciplinarity, this class of materials attracted the attention of a large number of researchers and originated in the beginning of a revolution in "Organic Electronics". Originating with an initial focus on the p- and n-doping of conjugated oligomers and polymers, the unique electrochemical behavior of these technological important materials enabled the development of cheap sensors. Because of the progress toward better developed materials with higher order and purity, these organic materials are now also available for "organic electronic" devices. More generally, organic electronics includes now diodes, photodiodes, photovoltaic cells, light emitting diodes, lasers, field effect transistors, electro-optical couplers and all organic integrated circuits and claims thereupon for key technology of the 21th century [1–3].

The area of conjugated organic semiconductors can be divided conditionally into two large parts: conjugated polymers and small conjugated organic molecules. Conjugated polymers combine properties of classical semiconductors with the inherent processing advantages of plastics and therefore play a major role in low cost, large area optoelectronic applications [4–6]. Unfortunately, polymer films are commonly highly disordered in the solid state and, consequently, show low charge carrier mobilities because of strong Anderson localization [7]. Therefore, an inherent part of research in the field of organic electronics focuses on small molecule systems, in which highly ordered crystalline structures can be achieved — in contrast to the disordered, often amorphous phases of the polymers. These molecules are additionally thermally stable up to 300–400°C, can be obtained as pure materials and processed in high-vacuum or ultra high-vacuum conditions [8–9]. The recent demonstration of effective optoelectronic devices based on molecular single-crystals like pentacene or C_{60} [10,11] has clearly shown the advantages of this "small molecule approach" and has received widespread attention. Further development of such devices requires obligatory the use of epitaxially grown highly cystalline thin films with well-defined orientation of the molecules. Unfortunately, up to now the physical properties of molecular thin films do not compare favorable to those of single-crystal materials. There is a large number of papers about significant influence of structural order on the performance of thin film devices based on small molecules [12,13]. In particular, the recent emphasis in research of conjugated oligomer films is founded in the correlation between the electronic structure [14] and charge transport through the active layer [15]. These studies are motivated by their implications on charge transport in organic field effect transistors (OFETs). It has been demonstrated (mostly for α-sexithiophene films) that the carrier mobility in OFETs can be significantly improved if the degree of order in all the film increases [16]. The correlation between degree of order and carrier mobility was also found for thin film structures based on other molecules [17]. High

order, implying enhanced charge carrier transport are also of major importance in other organic electronic devices: photodetectors and photovoltaic devices [18,19] and LEDs [20].

In addition to chances in device performance, well-ordered or single-crystalline molecular films allow the investigation of anisotropic optical and electronic properties of π-conjugated systems [21,22] as it was found in bulk crystals [8–11]. It should be mentioned here that such phenomena are commonly not observed in conjugated polymer thin films, which are usually disordered. Therefore, such investigations are also of considerable fundamental interest. The challenging task for the future is to grow epitaxial layers of high crystalline quality. The main difference between organic and inorganic materials with respect to epitaxial growth is the different nature of bonds. The inorganic materials are first physisorbed and then chemisorbed on the growing surface. In the case of organic materials only physisorbtion occurs because no chemical bonds are formed between the molecules. As a result, the growth process is governed by very weak bonds of Van der Waals' type reflected by a very small sticking coefficient. That means that epitaxial growth of organic materials is performed usually at comparable low temperatures. Many attempts were made so far to grow organic materials on inert surfaces mainly by MBE. An extended overview can be found in Ref. [23] MBE as growth method offers the advantage of *in situ* monitoring. On the other hand growth occurs in an open system far away from thermodynamic equilibrium. Especially in the case of Van der Waals epitaxy it is a distinct advantage to use a growth method which works as close as possible to thermodynamic equilibrium, which allows to grow at relatively high vapor pressures of the organic material in the region of the substrate where the deposition occurs.

2. EXPERIMENTAL SETUP

A growth method which satisfies the conditions for Van der Waals Epitaxy is the so called Hot-Wall-Beam Epitaxy (HWBE)[24]. In contrast to an Molecular Beam Epitaxy (MBE) system, HWBE uses the near field distribution of effusing molecules at the orifice of an effusion cell [25]. The substrate can also be used to close the tube of the source like a lid forming a semiclosed growth system, which is then known as Hot-Wall Epitaxy (HWE) [26]. HWE is proved as a very successful growth method for organic materials like C_{60} [27,28] and its Ba-containing compounds [29]. A quartz tube, with the source material at the bottom and the substrate on the top closing it tight with respect to the mean free path of the evaporated source molecules, is placed with three separated heaters into a high-vacuum

chamber. The region of the growth reactor between source and substrate, called hot wall, guarantees a nearly uniform and isotropic flux of the molecules onto the substrate surface. The advantage of such closed system is the minimization of source material losses, which can be very important in case of new organic materials which are not commercially available. To perform the doping experiments with Ba a slight modification of the HWE system was necessary to add to the usual growth reactor a second eva-poration source for doping material. A schematic cross-section of the improved HWE system can be seen in Figure 1 together with a typical temperature profile along the quartz tube. The Ba doping source is con-tained in a concentric quartz ampoule and heated separately by oven 2. In that way the partial pressure of C_{60} and Ba could be controlled indepen-dently. The used C_{60} source material was at first 99.4% pure. It had to be cleaned from solvents and impurities by subliming the material three times at 550°C under dynamical vacuum of 1×10^{-6} mbar and by protecting it from visible light in order to minimize photo-induced polymerization. About 200 mg of the cleaned material was loaded into the HWE system, which was enough to fabricate more than 50 epilayers with an area of $1 \, cm^2$ and an average thickness of 200 nm. The Ba-doping material was loaded in a glove box under nitrogen atmosphere into the quartz ampoule to avoid any oxidation.
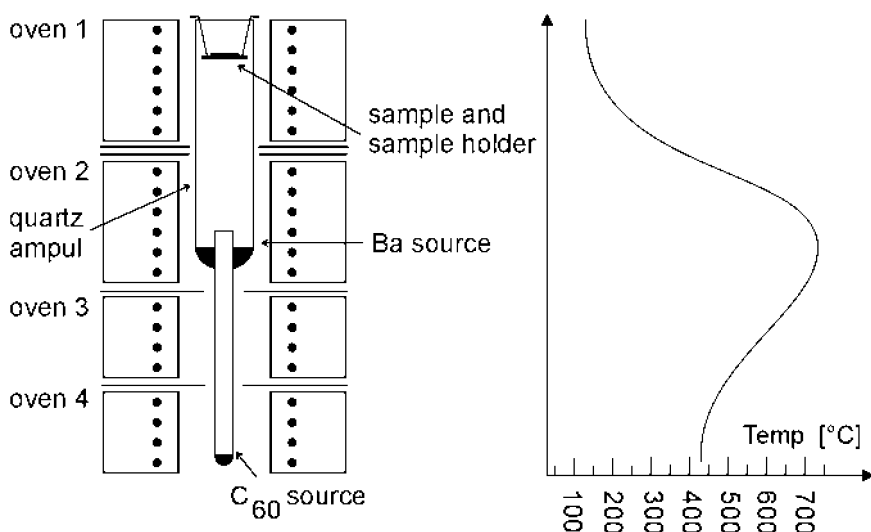
FIGURE 1 Schematic cross section of the HWE reactor to grow Ba-doped C_{60} films together with a typical temperature profile.

As substrate material, sheets of mica were used because of the inert character of freshly cleaved surfaces, free of unsaturated bonds which is in favor for Van der Waals Epitaxy. The top most layer of mica consists of Ka atoms forming a hexagonal grid with a periodicity which is close to the diameter of C_{60} molecules. Consequently epitaxial growth of C_{60} on mica should be initiated in the (111) direction. The mica sheets were cut into pieces ($15 \times 15 \, mm^2$), cleaved in air with an adhesive tape, and immediately transferred into the vacuum chamber of the HWE system. The substrates, before being transferred into the growth reactor, were preheated in the HWE chamber for 1 h at 400°C in a separate oven to remove adhesives from the substrate surface.

To grow pristine C_{60} epilayers, the substrate temperature was varied from 100°C to 200°C, and the wall temperature from 340°C to 440°C. Out of this wide range of temperatures a set was selected which gave the best crystalline quality. The influence of the substrate temperature on the growth and crystalline quality of C_{60} films was studied by varying the substrate temperature at a fixed source and wall temperature of 400°C.

3. RESULTS AND DISCUSSION

The FWHM of the x-ray rocking curves was used as criterion for crystalline quality.

In Figure 2, the rocking curve FWHM of the (111) reflex of C_{60} films, which are about 120 nm thick, is plotted as a function of T_{sub}. Regarding temperatures between 100°C and 200°C, the C_{60} film grown at 140°C has
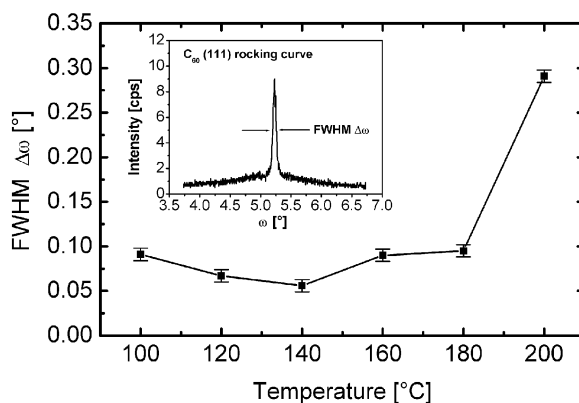

FIGURE 2 FWHM of the C_{60}(111) rocking curve versus the applied substrate temperature.

a minimal FWHM of 200 ± 20 arcs, indicating an nearly perfect mono-crystalline growth. For lower temperatures, there is a gentle increase of the FWHM, whereas for higher temperatures, a significant jump can be observed between 180°C and 200°C. The 120 nm thick films grown at T_{sub} between 100°C and 180°C exhibit a narrow Gaussian shape as shown in the inset of Figure 2.

The additional installed annealing oven allowed to perform post growth annealing processes without breaking the vacuum. The improvement in crystalline quality of the C_{60} epilayers by annealing was investigated by HRXD. Typical rocking curves of an as-grown and an annealed C_{60} layer of the same thickness of 100 nm are compared in Figure 3. The FWHM of the as-grown layer is 240 arcs, comparable with the results reported above. The improvement of the annealed layer, which was baked 20 min at a temperature of 130°C, is documented by the decrease of the FWHM to 140 arcs and the increase of the peak intensity. The crystalline quality of the annealed C_{60} was also tested by pole-figure measurements. Six sharp maxima indicated twin formation, however, the sharpness of the peaks, and the very low background signal were a clear indication of the high crystalline quality.

For all doping experiments, the C_{60} source temperature and the substrate temperature were kept constant at 400°C and 140°C, respectively. To study the incorporation of Ba we varied the Ba source temperature between 470°C and 750°C, resulting in Ba_xC_{60} compound layers.
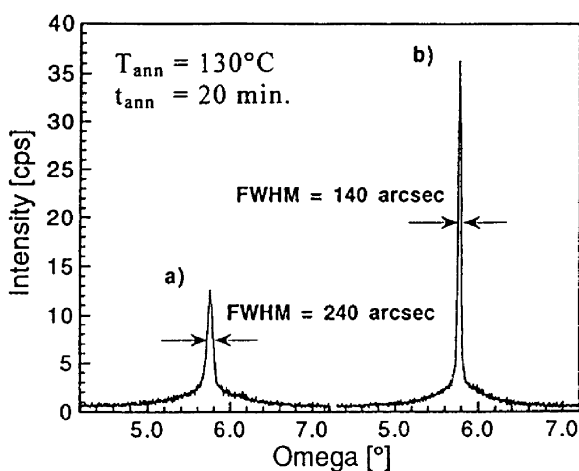
FIGURE 3 X-ray rocking curve for (a) as-grown and (b) annealed C_{60} layers. The annealing time and temperature are inserted.
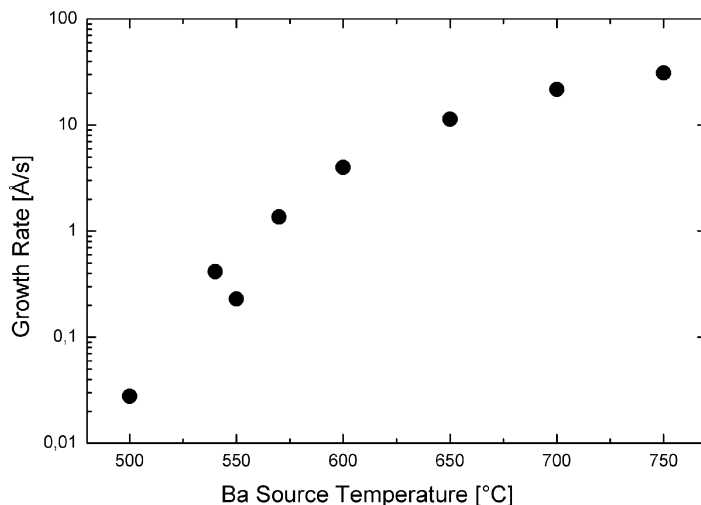
FIGURE 4 Growth rate of the Ba-doped C_{60} layers as a function of the Ba source temperature.

It is very important to notice that as soon as Ba was used in the growth reactor, the growth rate of the C_{60} layers was mainly controlled by the Ba source temperature and only slightly dependent on the C_{60} vapor pressure. Figure 4 shows the average growth rate of Ba-doped C_{60} layers which were grown for 7 h. For Ba source temperatures smaller than 600°C, the results follow an exponential function: for higher Ba temperatures a saturation can be observed. This behavior can be interpreted by the assumption that the incorporated Ba causes a charge transfer to C_{60}[30] and controls the sticking coefficient for the C_{60} molecules that are always present in a surplus in the vapor. However, when the surface coverage of Ba is saturated, the growth rate also cannot be increased further. In that way the growth mechanism changes from Van der Waals Epitaxy, which is typical of pure fullerenes, to a different mechanism resulting from a stronger bonding type evoked by the charge transfer.

The resistivity of the Ba-doped layers was measured *in situ* by a four-point probe without breaking the vacuum. We found, that the resistivity depends only on the applied Ba source temperature. For Ba source temperatures smaller than 600°C an exponential decrease of the resistvity can be observed. For larger Ba source temperatures a saturation is observed. We conclude, that for Ba source temperatures larger than 600°C the growing surface is saturated with Ba atoms and consequently no further incorporation and decrease in resistivity can be achieved. It is worthwhile to notice, that the growth rate (Fig. 3) and the resistivity (Fig. 4) show the

same trends. For Ba source temperatures below 520°C the growth rate and the resistivity are comparable to pristine C_{60} layers, which means, that the Ba partial pressure is to low to obtain an effective Ba incorporation, and consequently no charge transfer occurs, resulting in an increase of growth rate or decrease of resistivity. Also the typical saturation behavior is observed in growth rate and resistivity as we beyond Ba source temperatures of 600°C, which can be interpreted as a limitation in the Ba incorporation rate at electrical active sites.

Nothing was known so far about the carrier concentration or the mobility of carriers in Ba containing C_{60} layers. We installed a permanent magnet with a magnetic field of 0.43 Tesla in the vacuum chamber of the HWE system and realized the possibility of measuring Hall effect on Ba_xC_{60} epilayers. The sample holder with the necessary wiring and the contacted Ba_xC_{60} layer could be transferred from the HWE growth reactor to the permanent magnet. The evaluation of the data gave n-type conductivity with a carrier concentration between $10^{13}-10^{18}\,cm^{-3}$. For Ba source temperatures larger than 600°C the carrier concentration saturated around $2 \times 10^{18}\,cm^{-3}$, which fits very well into the picture obtained from the growth rate and the resistivity measurements.

Even more surprising were the data obtained for the mobility of the carriers that are much higher than expected. The mobility measured for each sample is shown in Figure 5 as a function of the obtained carrier
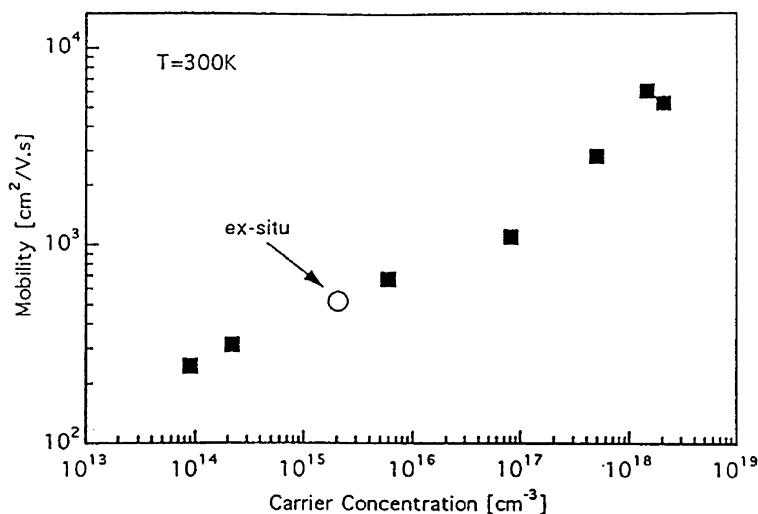
FIGURE 5 Carrier mobility as a function of n-type carrier concentration. For comparison the *ex-situ* measured data point is given by an open circle.

concentration. The maximum measured mobility was $6000\,\mathrm{cm^2/Vs}$, which is to our knowledge the largest mobility reported in literature so far. To verify our experimental results we performed in addition to the Hall effect measurements magneto resistance measurements, which gave in all experiments the same results within an experimental error of 5% in comparison to the data obtained from hall effect.

To prove our *in situ* measurements we fabricated a sandwich structure by covering the Ba_xC_{60} with pristine C60. So we could expose this sandwich structure to ambient air and transfer the layer to a standard *ex-situ* Hall effect equipment. The obtained result is shown in Figure 5 labeled with "*ex-situ*". The excellent alignment with the data obtained from *in-situ* measurements was very convincing for the reliability of the data obtained before.

4. CONCLUSIONS

We have shown, that HWE is an appropriate method for growing C_{60} and Ba doped C_{60} epilayers. The excellent crystalline quality of the epilayers could be further improved by *in-situ* annealing processes, resulting in a FWHM of the X-ray rocking curve of 140 arcsec.

The incorporation of Ba in the C_{60} layers caused a significant charge transfer from the Ba atoms to the C_{60} molecules, resulting in an increase of the growth rate and an n-type conductivity of the doped layers with enormously high mobility of the charge carriers.

REFERENCES

[1] Heeger, A. J. (2001). *Current Appl. Phys.*, *1*, 247.
[2] McGehee, M. D., Miller, E. K., Moses, D., & Heeger, A. J. (1999). Twenty years of progress in science and technology. In: P. Bernier, S. Lefraut, & G. Bidan (Eds.), *Advances in Synthetic Metals*, Elsevier: Lausanne.
[3] McGehee, M. D., & Heeger, A. J. (2000). *Adv. Mat.*, *12*, 1655.
[4] Burroughes, J. H., Bradley, D. D. C., Brown, A. R., Marhus, R. N., Mackay, K., Friend, R. H., Burn, P. L., Kraft, A., & Holmes, A. B. (1990). *Nature*, *347*, 539.
[5] Granström, M., Harrison, M. G., & Friend, R. H. (1999). In: D. Fichou (Ed.), *Handbook of Oligo- and Polythiophenes*, (p. 405ff). Weinheim: Wiley-VCH.
[6] Shaheen, S. E., Brabec, C. J., Sariciftci, N. S., Padinger, F., Fromherz, T., & Hummelen, J. C. (2001). *Appl. Phys. Lett.*, *78*, 841.
[7] Katz, H. E., Dodabalapur, A., & Bav, Z. (1999). In: D. Fichou (Ed.), *Handbook of Oligo- and Polythiophenes*, (p. 459ff). Weinheim: Wiley-VCH.
[8] Schön, J. H., Berg, S., Kloc, Ch., & Batlogg, B. (2000). *Science*, *287*, 1022.
[9] Schön, J. H., Kloc, Ch., Dodabalpur, A., & Batlogg, B. (2000). *Science*, *289*, 599.
[10] Schön, J. H., Kloc, Ch., & Batlogg, B. (2000). *Nature*, *408*, 549.
[11] Schön, J. H., Kloc, Ch., Bucher, E., & Batlogg, B. (2000). *Nature*, *403*, 408.

[12] Fichou, D., & Ziegler, C. (1999). In: D. Fichou (Ed.), *Handbook of Oligo- and Poly-thiophenes*, (p. 183ff). Weinheim: Wiley-VCH.

[13] Schön, J. H., Kloc, Ch., Landise, R. A., & Batlogg, B. (1998). *Phys. Rev. B*, *58*, 12952.

[14] Taliani, C., & Gebauer, W. (1999). In: D. Fichou (Ed.), *Handbook of Oligo- and Poly-thiophenes*, (p. 361ff). Weinheim: Wiley-VCH.

[15] Gundlach, D. J., Liu, Y.-Y., Jackson, T. N., & Schlom, D. G. (1997). *Appl. Phys. Lett.*, *71*, 3853.

[16] Dimitrakopoulos, C. D., & Malenfant, P. R. L. (2002). *Adv. Mat.*, *14* (2), 99.

[17] Katz, H. E., Lovingre, A. J., Johnson, J., Kloc, C., Slegrist, T., Li, W., Lin, Y.-Y., & Dodalapur, A. (2000). *Nature*, *404*, 478.

[18] Videlot, C., Fichou, D., & Garnier, F. (1999). *Synth. Met.*, *101*, 618.

[19] Videlot, C., & Fichou, D. (1999). *Synth. Met.*, *102*, 885.

[20] Yanagi, H., & Okamoto, S. (1997). *Appl. Phys. Lett.*, *71*, 2563.

[21] Andreev, A., Matt, G., Brabec, C. J., Sitter, H., Badt, D., Seyringer, H., & Sariciftci, N. S. (2000). *Adv. Mat.*, *12* (9), 629.

[22] Yanagi, H., Morikawa, T., Hotta, S., & Yase, K. (2001). *Adv. Mat.*, *13* (5), 313.

[23] Koma, A. (1995). *Prog. Cryst. Growth and Charact.*, *30*, 129.

[24] Humenberger, J., Gresslehner, K. H., Schirz, W., Sitter, H., & Lischka, K. (1991). *Mat. Res. Soc. Symp. Proc.*, *216*, 53.

[25] Humenberge, J., & Sitter, H. (1989). *Thin Solid Films*, *163*, 241.

[26] Lopez-Otero, A. (1978). *Thin Solid Films*, *49*, 3.

[27] Stifter, D., & Sitter, H. (1995). *Appl. Phys. Lett.*, *66*, 679.

[28] Stifter, D., & Sitter, H. (1996). *Fullerene Sci. and Technol.*, *4* (2), 277.

[29] Sitter, H., Stifter, D., & Nguyen Manh, T. (1997). *Thin Solid Films*, *306*, 313.

[30] Oshiyama, A., Saito, S., Hamada, N., & Miyamoto, Y. (1992). *J. Phys. Chem. Solids*, *53*, 1457.